Ca^{2+} waves in keratinocytes are transmitted to sensory neurons: the involvement of extracellular ATP and $P2Y_2$ receptor activation

Schuichi KOIZUMI*, Kayoko FUJISHITA†, Kaori INOUE‡, Yukari SHIGEMOTO-MOGAMI†, Makoto TSUDA† and Kazuhide INOUE†§[1]

*Division of Pharmacology, National Institute of Health Sciences, 1-18-1 Kamiyoga, Setagaya, Tokyo 158-8501, Japan, †Division of Biosignaling, National Institute of Health Sciences, 1-18-1 Kamiyoga, Setagaya, Tokyo 158-8501, Japan, ‡Shiseido Research Center, 2-12-1 Fukuura, Kanazawa-ku, Yokohama 236-8643, Japan, and §Graduate School of Pharmaceutical Sciences, Kyushu University, 3-1-1 Maidashi, Fukuoka 812-8582, Japan

ATP acts as an intercellular messenger in a variety of cells. In the present study, we have characterized the propagation of Ca^{2+} waves mediated by extracellular ATP in cultured NHEKs (normal human epidermal keratinocytes) that were co-cultured with mouse DRG (dorsal root ganglion) neurons. Pharmacological characterization showed that NHEKs express functional metabotropic $P2Y_2$ receptors. When a cell was gently stimulated with a glass pipette, an increase in $[Ca^{2+}]_i$ (intracellular Ca^{2+} concentration) was observed, followed by the induction of propagating Ca^{2+} waves in neighbouring cells in an extracellular ATP-dependent manner. Using an ATP-imaging technique, the release and diffusion of ATP in NHEKs were confirmed. DRG neurons are known to terminate in the basal layer of keratinocytes. In a co-culture of NHEKs and DRG neurons, mechanical-stimulation-evoked Ca^{2+} waves in NHEKs caused an increase in $[Ca^{2+}]_i$ in the adjacent DRG neurons, which was also dependent on extracellular ATP and the activation of $P2Y_2$ receptors. Taken together, extracellular ATP is a dominant messenger that forms intercellular Ca^{2+} waves in NHEKs. In addition, Ca^{2+} waves in NHEKs could cause an increase in $[Ca^{2+}]_i$ in DRG neurons, suggesting a dynamic cross-talk between skin and sensory neurons mediated by extracellular ATP.

Key words: ATP, Ca^{2+} wave, cross-talk, dorsal root ganglion neuron, keratinocyte, $P2Y_2$ receptor.

INTRODUCTION

The skin is the largest organ of the body and is exposed to multiple external stimuli. It protects water-rich internal organs from harmful environmental factors such as dryness, chemicals, noxious heat and UV irradiation. In addition, the skin is exposed to various substances such as ATP, bradykinin and histamine after skin injury and during inflammatory skin diseases and allergic reactions respectively. Thus the skin expresses various sensors for environmental stimuli [1,2] or neurotransmitters [3–6]. Various environmental stimuli or neurotransmitters often cause changes in $[Ca^{2+}]_i$ (intracellular Ca^{2+} concentration) in the skin [5,7,8]. Ca^{2+} dynamics play an important role in the homoeostasis of the skin epidermis, the outermost part of skin tissue; the skin epidermis tunes the balance between the proliferation and differentiation of epidermal keratinocytes [1,9].

Propagation of intercellular Ca^{2+} waves from one cell to another is a well-known phenomenon in non-excitable cells such as astrocytes [10,11], hepatocytes [12], epithelial cells [13] and endothelial cells [14]. These cells lack regenerative electrical action potentials but use Ca^{2+} waves for their long-range communications. In astrocytes, extracellular molecules such as glutamate [11] and ATP [15], rather than gap junction via connexin43, have been suggested to be important factors for the Ca^{2+} wave [16]. Epidermal keratinocytes are non-excitable cells and do not produce action potentials. However, the mechanisms of intercellular Ca^{2+} waves in keratinocytes have received only limited attention. Given that Ca^{2+} waves in keratinocytes are mediated by the release of extracellular molecules, such signals may also affect the activity of surrounding cells such as sensory neurons. Although junctions have not been found between keratinocytes and sensory termini, ultrastructural studies have shown that keratinocytes contact DRG (dorsal root ganglion) nerve fibres through membrane–membrane apposition [17,18]. Immunostaining of the neuronal marker PGP 9.5 (protein gene product 9.5) revealed the presence of free nerve endings at epidermal keratinocytes [19]. There is indirect evidence that keratinocytes communicate with sensory neurons via extracellular molecules. For example, although dissociated DRG neurons can be directly activated by heat and cold, warm responses have only been demonstrated in experiments where skin–nerve connectivity is intact [20,21]. A warmth sensor, TRPV3, is present in epidermal keratinocytes, but not in sensory neurons [19]. Sensory neurons themselves sense various external stimuli, but there might be skin-derived regulatory mechanisms by which sensory signalling is modulated.

In the present study, we report that mechanical stimulation of NHEKs (normal human epidermal keratinocytes) with a glass pipette induces propagating Ca^{2+} waves in an extracellular ATP-dependent manner. NHEKs release ATP and, in turn, the released ATP activates $P2Y_2$ receptors in NHEKs. We also demonstrate that, in a co-culture of NHEKs and DRG neurons, such extracellular ATP-dependent Ca^{2+} waves in NHEKs cause increases in $[Ca^{2+}]_i$ even in the adjacent DRG neurons, suggesting that dynamic cross-talk occurs between keratinocytes and DRG neurons via extracellular ATP.

EXPERIMENTAL

Cell culture

NHEKs were obtained as cryopreserved first passage cells from neonatal foreskins (Kurabo, Osaka, Japan). Cells were plated on collagen-coated coverslips and then cultured in serum-free

Abbreviations used: ATPγS, adenosine 5′-[γ-thio]triphosphate; BSS, balanced salt solution; $[Ca^{2+}]_i$, intracellular Ca^{2+} concentration; DRG, dorsal root ganglion; $\alpha\beta$meATP, α,β-methylene-ATP; 2meSADP, 2methyl-thio-ADP; NHEK, normal human epidermal keratinocyte; RT, reverse transcriptase.

[1] To whom correspondence should be addressed (e-mail inoue@nihs.go.jp).

keratinocyte growth medium consisting of Humedia-KB2 (Kurabo), supplemented with bovine pituitary extract (0.4 %, v/v), human recombinant epidermal growth factor (0.1 ng/ml), insulin (10 μg/ml), cortisol (0.5 μg/ml), gentamicin (50 μg/ml) and amphotericin B (50 ng/ml). The media were replaced every 2–3 days. For co-culturing NHEKs and mouse DRG neurons, NHEKs were seeded on mitomycin C (4 μg/ml)-treated 3T3-J2 fibroblast feeder layers (2×10^5 cells/cm^2) in 'Green' medium [3:4 Dulbecco's minimal Eagle's medium and 1:4 Ham's F12, supplemented with 10 % (v/v) foetal bovine serum, 20 mM Hepes, 100 units/ml penicillin, 100 μg/ml streptomycin, 5 μg/ml insulin, 0.5 μg/ml cortisol, 0.1 nM cholera enterotoxin, 0.01 μg/ml recombinant human epidermal growth factor, 0.25 μg/ml amphotericin B and 180 μM adenine]. The dissociated mouse DRG neurons were seeded, 2 days after the seeding of NHEKs, on the cell layer and then cultured for an additional 1 week.

Ca^{2+} imaging in single NHEKs

Changes in $[Ca^{2+}]_i$ in single cells were measured by the fura 2 method as described by Grynkiewicz et al. [22] after minor modifications [23]. In brief, the culture medium was replaced with BSS (balanced salt solution) of the following composition (mM): NaCl 150, KCl 5.0, $CaCl_2$ 1.8, $MgCl_2$ 1.2, Hepes 25 and D-glucose 10 (pH 7.4). Cells were loaded with fura 2 by incubation with 5 μM fura 2/AM (fura 2 acetoxymethyl ester; Molecular Probes, Eugene, OR, U.S.A.) at room temperature (20–22 °C) in BSS for 45 min, followed by washing with BSS and a further 15 min incubation to allow de-esterification of the loaded dye. The coverslips were mounted on an inverted epifluorescence microscope (TMD-300; Nikon, Tokyo, Japan) equipped with a 75 W xenon lamp and band-pass filters of 340 and 360 nm wavelengths. Measurements were carried out at room temperature. Images were recorded by a high-sensitivity silicon intensifier target camera (C-2741-08; Hamamatsu Photonics, Hamamatsu, Japan) and the image data were regulated by a Ca^{2+} analysing system (Furusawa Laboratory Appliance, Kawagoe, Japan). The absolute $[Ca^{2+}]_i$ was estimated from the ratio of emitted fluorescences (F_{340}/F_{360}) according to a calibration curve obtained by using Ca^{2+} buffers. For Ca^{2+}-free experiments, Ca^{2+} was removed from the BSS (0 Ca^{2+}). Drugs were dissolved in BSS and applied by superfusion. For mechanical stimulation, a single NHEK in the centre of the microscopic field was probed with a glass micropipette using a micromanipulator (Narishige, Tokyo, Japan). Under visible light, the tip of the micropipette was positioned approx. 2 μm over the cell to be stimulated. When sampling, the micropipette was rapidly lowered by approx. 2 μm and then rapidly returned to its original position. If the stimulated cell showed no increase in fluorescence, the pipette was lowered again until stimulation was seen. If the stimulated cell showed any sign of damage (dye leakage or abnormal morphology), the experiment was eliminated. For confocal Ca^{2+} imaging, the cells were loaded with 5 μM fura 4/AM for 30–40 min at room temperature and then mounted on a microscope (TE-2000; Nikon) equipped with a CSU-10 laser-scanning unit (Yokogawa, Tokyo, Japan) and a high-sensitivity CCD (charge-coupled-device) camera (ORCA-ER; Hamamatsu Photonics), as described previously [24]. To compensate for the uneven distribution of the fluo-4, self-ratios were calculated ($R_s = F/F_0$), which were subsequently converted into Ca^{2+} concentration using the following equation:

$$[Ca^{2+}]_i = R_s K_d / [(K_d / [Ca^{2+}]_{rest}) - R_s]$$

The K_d value of fluo-4 for NHEKs was taken to be 706 nM as determined by an *in vivo* calibration method.

Table 1 Primer pairs and end-products

Amplicon shows the base pairs of the PCR end-product.

Gene	Primer	Size (-mer)	Amplicon (bp)
P2Y1	F: 5′-GAGGGCCCGGCTTGATT-3′	17	67
	R: 5′-ATACGTGGCATAAACCCTGTCA-3′	22	
P2Y2	F: 5′-TGGTGCGCTTCCTCTTCTACA-3′	21	72
	R: 5′-ACCGGTGCACGCTGATG-3′	17	
P2Y4	F: 5′-TCATGGCTCGTCGCCTGTA-3′	19	67
	R: 5′-AGAGAGCGGAGGCGAGAAG-3′	19	
P2Y6	F: 5′-CCTGCCCACAGCCATCTT-3′	18	116
	R: 5′-CAGTGAGAGCCATGCCATAGG-3′	21	
P2Y11	F: 5′-CTGCCCTGCCAACTTCTTG-3′	19	78
	R: 5′-ACCAGTATGGGCCACAGGAA-3′	20	
P2Y12	F: 5′-CCTTTCCATTTTGCCCGAAT-3′	20	74
	R: 5′-GTATTTTCAGCAGTGCAGTCAAAGA-3′	25	

Imaging of ATP release

ATP release from NHEKs was detected with a luciferin–luciferase bioluminescence assay. After an initial 30 min superfusion period, superfusion was stopped and the cell chamber was filled with BSS containing a luciferase reagent (ATP bioluminescence assay kit CLS II; Roche Diagnostics, Mannheim, Germany). ATP bioluminescence was detected and visualized with a VIM camera (C2400-35; Hamamatsu Photonics) using an integration time of 30 s. The absolute ATP concentration was estimated using a standard ATP solution (ATP bioluminescence assay kit CLS II).

Immunocytochemistry

Cultures were fixed with 4 % (w/v) paraformaldehyde for 10 min and soaked in PBS solution. Cells were incubated with primary antibodies (rabbit anti-peripherin antibody, 1:200; Chemicon, Temecula, CA, U.S.A.; monoclonal mouse anti-cytokeratin14 antibody, 1:100; Cymbus Biotechnology, Chandlers Ford, U.K.), dissolved in blockace solution (1:10 dilution; Dainippon, Osaka, Japan) for 1 h at room temperature and then covered with diluted (1:500) secondary fluorescent antiserum solution (Alexa488- and Alexa546-conjugated rabbit and mouse anti-IgGs respectively) and kept at 4 °C overnight. Then, the cells were washed three times with PBS containing 0.05 % Tween 20 for 15 min and mounted with Vectashied (Vector Laboratories, Burlingame, CA, U.S.A.). Images were obtained by confocal microscopy (Radiance 2000; Bio-Rad Japan, Tokyo, Japan).

Reverse transcriptase (RT)–PCR of P2 receptors

The total RNA was isolated and purified using RNeasy mini kits (Qiagen) according to the manufacturer's instructions. RT–PCR amplifications were performed using Taqman One-step RT–PCR Master Mix Reagents and 200 nM of each P2 receptor-specific primer. Using the software Primer Express (Applied Biosystems, Tokyo, Japan), clone-specific primers were designed to recognize human P2Y receptors, as shown in Table 1. All primers had similar melting temperatures for running the same cycling programme for all samples. RT–PCR was performed by 30 min reverse transcription at 48 °C, 10 min AmpliTaq Gold activation at 95 °C, then 15 s denaturation at 95 °C and, finally, 1 min annealing and elongation at 60 °C for 40 cycles in a PRISM 7700 (Applied Biosystems). To exclude contamination by unspecific PCR products such as primer dimers, melting curve analysis was performed on all the final PCR products after the cycling procedure.

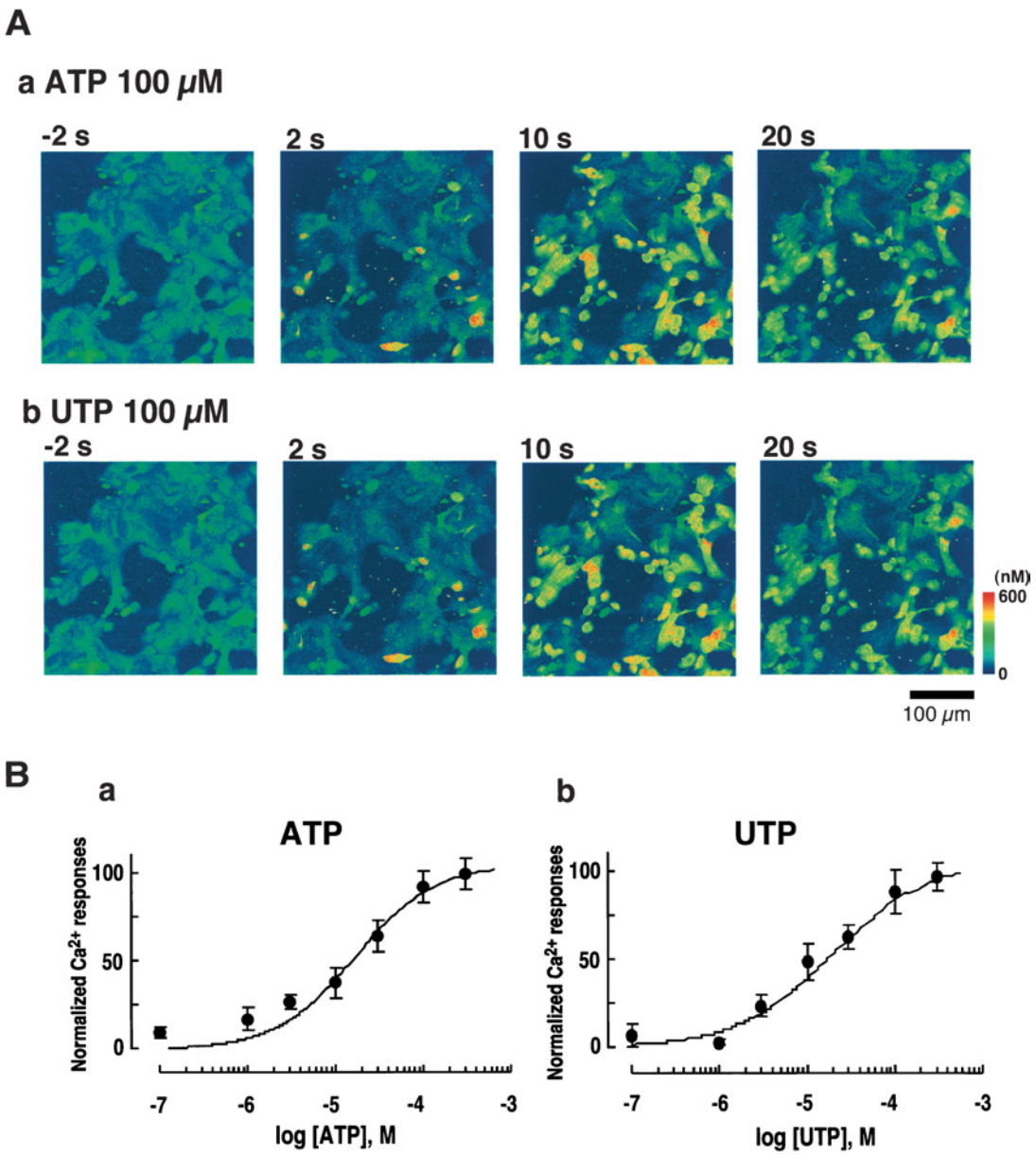

Figure 1 Increases in $[Ca^{2+}]_i$ evoked by both applied ATP and UTP in NHEKs

(**A**) Sequential pseudo colour images of Ca^{2+} responses to 100 μM ATP (**a**) and UTP (**b**). Images were obtained from a confocal laser microscope, showing self-ratios of fluo-4 fluorescence. Images were recorded 2 s before (−2 s) and 2, 10 and 20 s after ATP or UTP application. (**B**) Concentration–response curves for (**a**) ATP- and (**b**) UTP-evoked increases in $[Ca^{2+}]_i$ in NHEKs. Increases in $[Ca^{2+}]_i$ in NHEKs were monitored by ratiometric fura 2 fluorescence ($\Delta F_{340}/F_{360}$) and were then converted into absolute value of $[Ca^{2+}]_i$ using a standard calibration curve. The maximum $[Ca^{2+}]_i$ increase was observed when cells were stimulated with 300 μM ATP (**a**) or UTP (**b**). The increase in $[Ca^{2+}]_i$ at each ATP or UTP concentration was normalized by the maximum increase in $[Ca^{2+}]_i$. Results are the means ± S.E.M. for 28–73 cells tested. Both the ATP- and UTP-evoked concentration–response curves were almost identical with the ED_{50} values of 21 and 20 μM respectively.

Statistics

Experimental results are expressed as means ± S.E.M. and statistical differences between two groups were determined by Student's *t* test.

RESULTS

Characterization of ATP-evoked $[Ca^{2+}]_i$ increases in NHEKs

Exogenously applied ATP induced an increase in $[Ca^{2+}]_i$ in NHEKs with an ED_{50} value of 21 μM (Figures 1Aa and 1Ba). UTP also caused an increase in $[Ca^{2+}]_i$ in the cells, with a similar ED_{50} value of 20 μM (Figures 1Ab and 1Bb). The ATP-evoked increase in $[Ca^{2+}]_i$ was almost independent of the extracellular Ca^{2+}, but was decreased by U73122, an inhibitor of phospholipase C, and thapsigargin, an inhibitor of Ca^{2+}-ATPase of Ca^{2+} stores, suggesting the involvement of inositol 1,4,5-trisphosphate/phospholipase C-linked metabotropic P2Y receptors in the Ca^{2+} responses (Figure 2A). UTP activates UTP-preferring $P2Y_2$ and $P2Y_4$ receptors, and UDP, generated by de-phosphorylation of UTP, stimulates $P2Y_6$ receptors. We therefore analysed the expression of mRNAs for these P2Y receptors using an RT–PCR method and detected the signals for $P2Y_1$, $P2Y_2$ and $P2Y_{11}$ receptors (Figure 2B, inset). Each PCR product possessed the predicted length (Table 1). Signals for $P2Y_4$, $P2Y_6$ and $P2Y_{12}$ were hardly detected in NHEKs. To confirm the functional responses

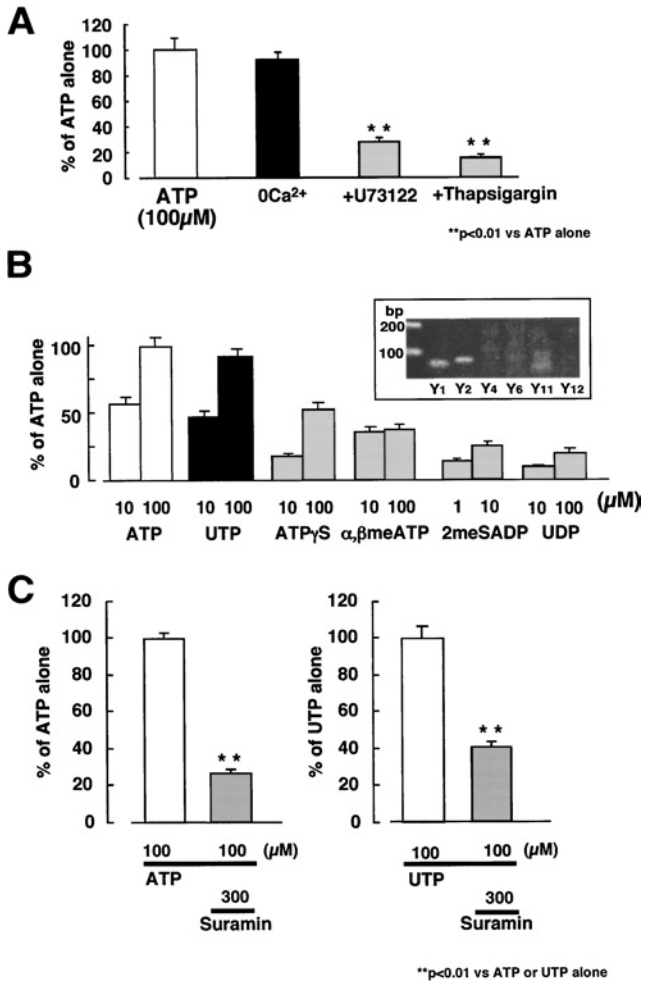

Figure 2 Characterization of P2 receptor-mediated Ca^{2+} responses in NHEKs

The ATP-evoked increases in $[Ca^{2+}]_i$ in NHEKs were characterized. Increases in $[Ca^{2+}]_i$ in cells were calculated by ratiometric fura 2 fluorescence ($\Delta F_{340}/F_{360}$) and a standard calibration curve. Values were normalized by the Ca^{2+} response at 100 μM ATP or UTP and were expressed as a percentage of ATP or UTP alone (**C**, right). (**A**) ATP was applied to NHEKs for 20 s and the U73122 (5 μM) was applied to the cells 10 min before and during the ATP application. Thapsigargin (100 nM) was applied to the cells 5 min before and during the ATP application. Results were obtained from 28 to 61 cells tested (at least two independent experiments). $^{**}P < 0.01$, significant differences from the response evoked by ATP alone. (**B**) Pharmacological characterization of Ca^{2+} responses in NHEKs. UTP was as potent as ATP. ATPγS and $\alpha\beta$meATP were much less potent than ATP. 2meSADP and UDP caused only slight increases in $[Ca^{2+}]_i$ in NHEKs. Results were obtained from 24 to 57 cells tested (at least two independent experiments). The inset shows the agarose-gel electrophoresis, indicating expression of mRNAs for various P2Y receptors in NHEKs. (**C**) Suramin (300 μM) inhibited both the ATP- and UTP-evoked increases in $[Ca^{2+}]_i$ in NHEKs. Results were obtained from 117 to 128 cells tested (four independent experiments). $^{**}P < 0.01$, significant differences from the response evoked by ATP or UTP alone.

of these P2Y receptors, we further performed pharmacological analysis using the fura 2-based Ca^{2+} imaging methods. The increase in $[Ca^{2+}]_i$ evoked by UTP was almost identical with that evoked by ATP. Both the $P2Y_{11}$ receptor agonist ATPγS (adenosine 5′-[γ-thio]triphosphate) and the P2X receptor agonist $\alpha\beta$meATP (α,β-methylene-ATP) caused increases in $[Ca^{2+}]_i$, but they were less than those caused by ATP or UTP. 2meSADP (2methyl-thio-ADP), a $P2Y_1$ receptor agonist, and UDP, a $P2Y_6$ receptor agonist, evoked only slight increases in $[Ca^{2+}]_i$ in the cells. The potency rank order for the Ca^{2+} response was ATP = UTP > ATPγS > $\alpha\beta$meATP > 2meSADP > UDP (Figure 2B). Cross-desensitization was observed between ATP and UTP (results not shown). Suramin at 300 μM decreased both the ATP- and UTP-evoked $[Ca^{2+}]_i$ increases (Figure 2C: 29.8 ± 2.2 % of ATP alone, $n = 128$; 44.1 ± 2.7 % of UTP alone, $n = 117$). These results suggest that the $P2Y_2$ receptors were responsible for these responses.

Propagating Ca^{2+} waves in response to mechanical stimulation in NHEKs

When an NHEK was stimulated with a glass pipette, an increase in $[Ca^{2+}]_i$ in the cell was observed, followed by induction of a propagating Ca^{2+} wave after a time lag in neighbouring NHEKs (Figure 3A, upper panels). The findings that the same cell evoked a Ca^{2+} response to repeated (up to three times) mechanical stimulations (results not shown) and that the cell showed some sign of damage suggest that mechanical stimulation would not cause injury to the stimulated cells. The propagation of Ca^{2+} waves was abolished by 80 units/ml apyrase [grade III; Figures 3A (lower panels) and 3B]. Both the P2 receptor antagonists suramin (300 μM) and pyridoxal phosphate-6-azophenyl-2′,4′-disulphonic acid (100 μM) significantly inhibited the Ca^{2+} wave; however, adenosine 3′-phosphate 5′-phosphosulphate (100 μM), an antagonist to the $P2Y_1$ receptor, and 1-octanol (500 μM), an inhibitor of gap junction, did not affect the Ca^{2+} waves (Figure 3C). The $[Ca^{2+}]_i$ increase in the stimulated cells was not affected by these antagonists. All these findings suggest that the propagating Ca^{2+} wave in response to mechanical stimulation in NHEKs was mediated by extracellular ATP and mainly by the activation of $P2Y_2$ receptors.

Release and diffusion of ATP from NHEKs

To demonstrate directly the stimulus-evoked release of ATP from NHEKs, we modified the luciferin–luciferase chemiluminescence bioassay for detecting ATP levels by using a high-sensitivity single photon-counting camera to correlate photon counts with increases in extracellular ATP. NHEKs were bathed in a solution containing the luciferin–luciferase reagents and photons were counted before and 30 s after mechanical stimulation of an NHEK. Figure 4(a) shows a phase-contrast image of a microscopic field, and Figures 4(b) and 4(c) show bioluminescence images before and after mechanical stimulation in the same field respectively. The standard calibration curve obtained under this condition showed a high correlation between the bioluminescence intensity and the ATP concentration with a correlation coefficient of 0.986 over a concentration range of 10 nM–10 μM (Figure 4d). The resting level of the bioluminescence signal was very low; then, it was increased to a level sufficient to evoke increases in $[Ca^{2+}]_i$ in NHEKs (3.2 ± 0.91 μM, $n = 12$) in response to mechanical stimulation for 30 s (Figures 4c and 4f). To visualize the spatiotemporal dynamics of the stimulus-evoked release of ATP from NHEKs, the extracellular ATP levels were plotted as pseudo colour images using the Excel 2-D surface plot program. As shown in Figures 4(e) and 4(f), the levels of extracellular ATP after mechanical stimulation were highest at the site of stimulation and decreased concentrically. These results show that the mechanically evoked Ca^{2+} waves were well associated with the release of ATP from NHEKs and the activation of $P2Y_2$ receptors.

Ca^{2+} waves in NHEKs activate increase in $[Ca^{2+}]_i$ in DRG neurons

As described in the Introduction section, sensory neurons terminate in the skin. Hence, a co-culture of NHEKs and mouse

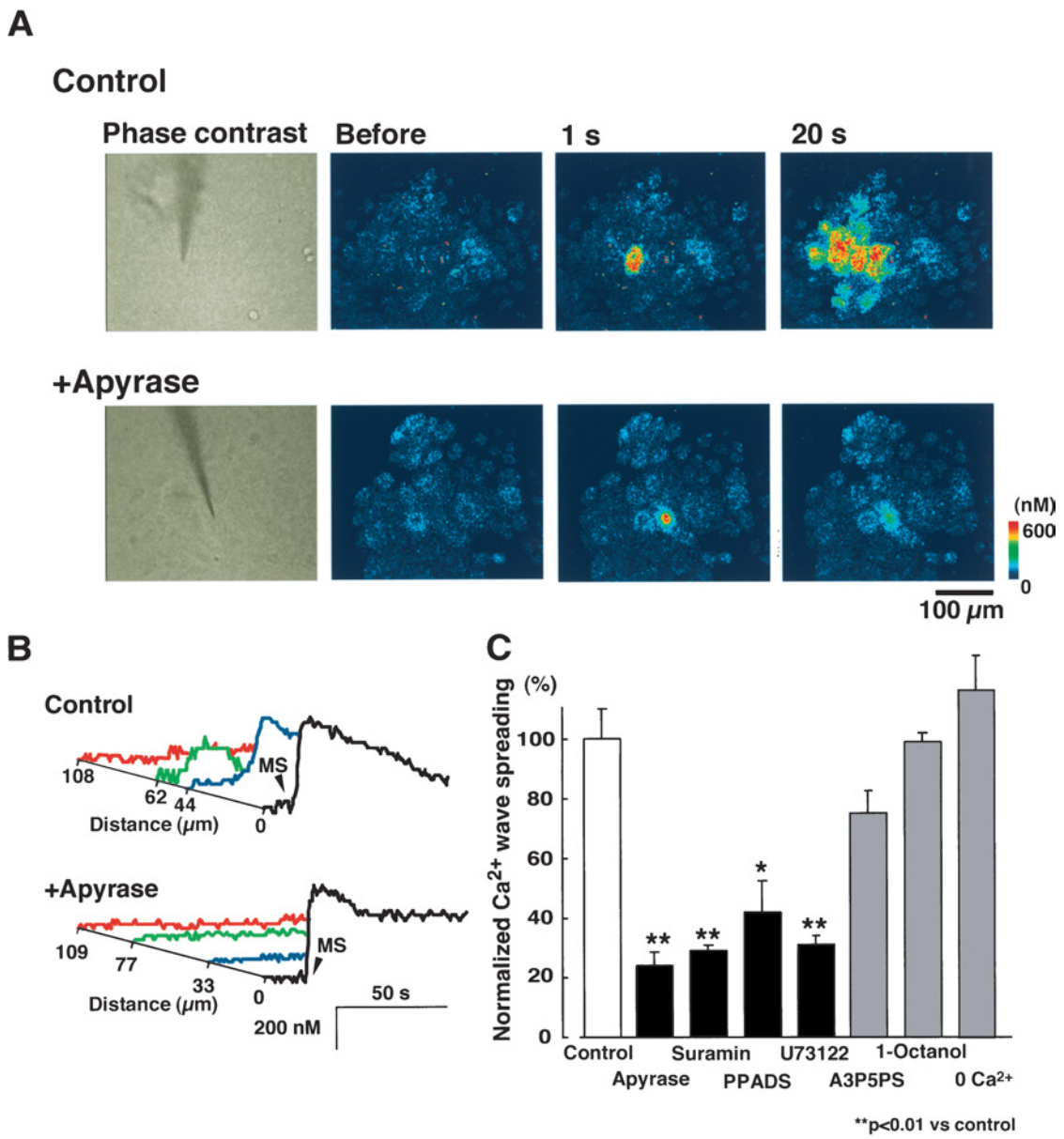

Figure 3 Propagation of Ca^{2+} waves in response to mechanical stimulation in NHEKs

(**A**) Phase-contrast (left) and pseudo $[Ca^{2+}]_i$ images of a field of cultured NHEKs in the absence (upper panels) and presence (lower panels) of apyrase (80 units/ml). Increase in $[Ca^{2+}]_i$ was estimated by ratiometric fura 2 fluorescence ($\Delta F_{340}/F_{360}$) and was then converted into absolute $[Ca^{2+}]_i$ using a standard calibration curve. A single NHEK was mechanically stimulated. (**B**) Plots of $[Ca^{2+}]_i$ as a function of time in four individual NHEKs in the microscopic field. The plots for the non-stimulated cells (blue, green and red traces) horizontally regressed in proportion to their distance from the stimulated cell (black traces) as indicated by the scale bar. In a control experiment, mechanical stimulation of NHEK 1 (black trace) resulted in the induction of a Ca^{2+} wave in adjacent cells after a time lag (upper traces). However, in the presence of apyrase (80 units/ml), mechanical stimulation failed to cause increases in $[Ca^{2+}]_i$ in the surrounding NHEKs (lower traces). The diameter of the spreading distance of the Ca^{2+} wave was calculated in the absence and presence of various chemicals and is summarized in (**C**). The average diameter of the Ca^{2+} wave under the control condition was 93.4 ± 9.7 μm ($n = 12$). Suramin (300 μM), pyridoxal phosphate-6-azophenyl-2′,4′-disulphonic acid (PPADS; 100 μM) and U73122 (5 μM) also abolished the propagation of Ca^{2+} waves, but adenosine 3′-phosphate 5′-phosphosulphate (A3P5PS; 100 μM), 1-octanol (500 μM) or removal of extracellular Ca^{2+} (0 Ca^{2+}) failed to inhibit the mechanical-stimulation-evoked Ca^{2+} wave in NHEKs ($n = 8$–12).

DRG neurons was prepared as described in the Experimental section. Figure 5(A) shows an immunohistochemical image of anti-cytokeratin14 (red) and anti-peripherin (green) antibodies, which are markers for the basal layer of keratinocytes and small-sized DRG neurons respectively. When stimulated with 80 mM KCl, almost all peripherin-positive DRG neurons (Figure 5B, green traces) exhibited increases in $[Ca^{2+}]_i$, whereas cytokeratin14-positive NHEKs (Figure 5B, red trace) did not. Both ATP (100 μM) and UTP (100 μM) caused increases in $[Ca^{2+}]_i$ in 71 % of the small-sized DRG neurons (37 out of 52 cells tested; $dF/F_0 = 6.3 \pm 0.8$ for ATP and 5.8 ± 0.6 for UTP; $n = 37$ in four separate experiments), and 73 % of NHEKs (58 out of 79 cells tested; $dF/F_0 = 5.1 \pm 0.7$ for ATP and 4.3 ± 0.4 for UTP; $n = 58$ in four separate experiments). The UTP-evoked increases in $[Ca^{2+}]_i$ in both types of cells were reproducible, and the first and second UTP-evoked responses were almost identical. The average diameter of the small-sized DRG neurons was 21.8 ± 3.5 μm. Suramin (100 μM) inhibited the UTP-evoked increases in $[Ca^{2+}]_i$ in both types of cells (DRG neurons, 10.2 ± 2.1 % of UTP alone, $n = 37$; NHEKs, 32.1 ± 4.6 % of UTP alone, $n = 58$). Thus

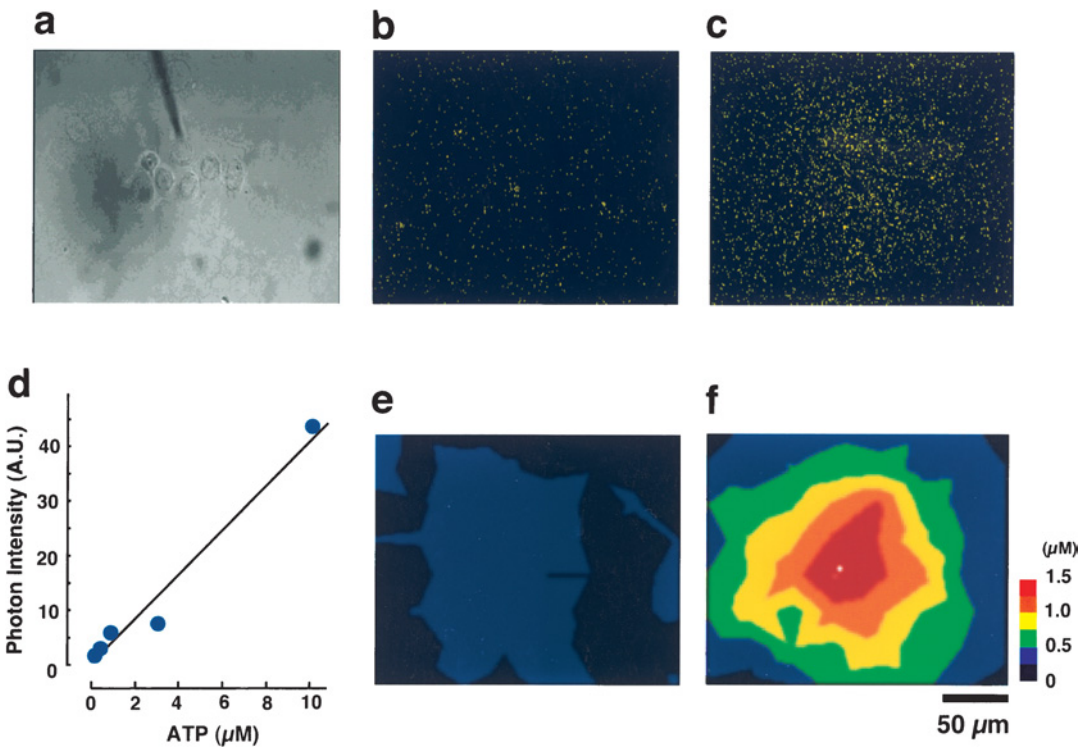

Figure 4 Visualization of release of ATP from NHEKs

The images show photon counts (yellow dots) in a field of NHEKs bathed in luciferin–luciferase reagent before (**b**) and after (**c**) mechanical stimulation. The position of pipette is shown in a phase-contrast image of NHEKs (**a**). (**d**) A typical bioluminescence intensity–ATP concentration relationship under these conditions. Various concentrations of ATP standard solution were injected in the presence of the luciferin–luciferase reagent, and photons were then accumulated for 30 s. (**e**, **f**) Spatial distribution of photon counts of mechanical stimulation shown as a two-dimensional pseudo colour surface plot. Scale bar, 50 μm for images **a**–**c**.

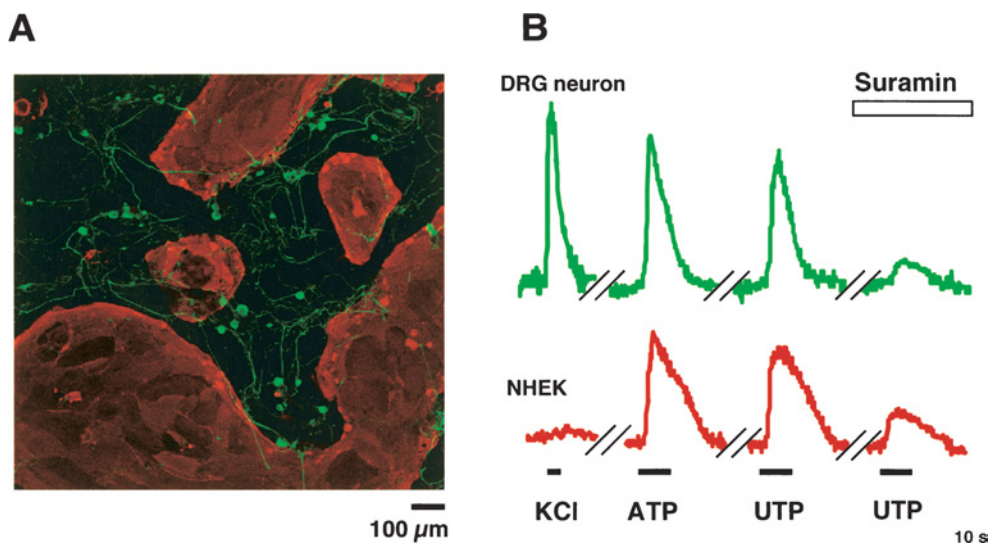

Figure 5 Immunohistochemical staining of DRG neurons and NHEKs

(**A**) After some Ca^{2+} imaging experiments, cells were fixed and stained with anti-cytokeratin14 and anti-peripherin antibodies for confirming NHEKs and small-sized DRG neurons respectively. (**B**) Representative Ca^{2+} responses obtained from self-ratios of fluo-4 fluorescence in anti-peripherin-positive DRG neuron (green) and anti-cytokeratin14-positive NHEK (red). First, cells were stimulated with 80 mM KCl for 3 s. Then, they were stimulated with 100 μM ATP for 10 s and 100 μM UTP for 10 s separated by 5 min. Finally, UTP (100 μM) was applied to the cells in the presence of 100 μM suramin. Both ATP and UTP caused increases in $[Ca^{2+}]_i$ in approx. 71 % of the DRG neurons (37 out of 52 cells tested) and in 73 % of the NHEKs (58 out of 79 cells tested) in the co-cultured cells.

most of the small-sized neurons also expressed UTP-preferring suramin-sensitive P2Y receptors, presumably $P2Y_2$ receptors. In the co-culture of NHEKs and DRG neurons, mechanical stimulation of a single NHEK produced a propagating Ca^{2+} wave in adjacent NHEKs in an extracellular ATP-dependent manner (Figure 6A). Interestingly, this Ca^{2+} wave in the NHEKs was

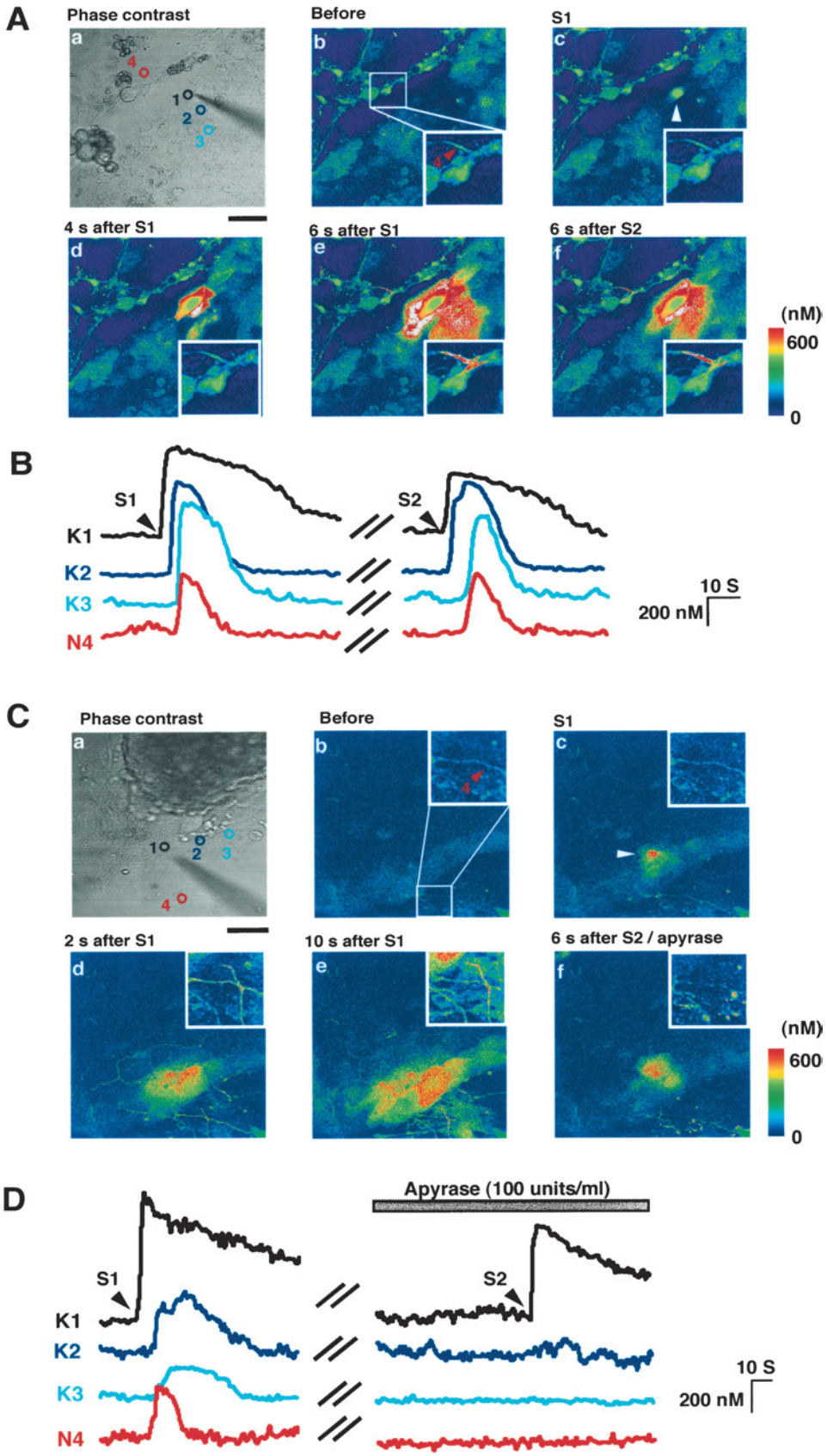

Figure 6 For legend see next page

followed by an increase in $[Ca^{2+}]_i$ in the DRG neurons after a time lag (Figures 6Ae and 6B, trace N4). The increases in $[Ca^{2+}]_i$ in DRG neurons were also dependent on extracellular ATP and the activation of P2 receptors, since the ATP-degrading enzyme, apyrase (grade III, 100 units/ml; Figures 6Cf and 6D), and suramin (100 μM) inhibited the increase in $[Ca^{2+}]_i$ (apyrase, 9.6 ± 0.9% of S1, $n = 21$; suramin, 14.8 ± 1.9% of S1, $n = 33$). Thus we concluded that the release of ATP in response to mechanical stimulation from NHEKs functions as an intercellular molecule between NHEKs and DRG neurons, which may affect nociceptive transduction in peripherin-positive neurons.

DISCUSSION

In the present study, we have demonstrated that ATP is a dominant extracellular signalling molecule in the formation of intercellular Ca^{2+} waves in NHEKs. We also showed that extracellular ATP-dependent Ca^{2+} waves in NHEKs caused increases in $[Ca^{2+}]_i$ in the adjacent DRG neurons. Thus ATP derived from NHEKs functions in both an autocrine and paracrine manner in the peripheral skin-to-sensory neuron system.

Both ATP and UTP caused increases in $[Ca^{2+}]_i$ in NHEKs to a similar extent. These Ca^{2+} responses were independent of extracellular Ca^{2+}, but dependent on inositol 1,4,5-trisphosphate-sensitive Ca^{2+} stores, suggesting the involvement of metabotropic P2Y receptors in the responses. ATP and UTP are natural ligands at $P2Y_2$ receptors, and are approximately equipotent. UTP also activates $P2Y_4$ receptors, but the human $P2Y_4$ receptor is highly selective for UTP than ATP [25]. UDP, an agonist to $P2Y_6$ receptors, only slightly increased the $[Ca^{2+}]_i$ in NHEKs [26,27]. Suramin moderately antagonizes human $P2Y_2$ receptors but not human $P2Y_4$ receptors [28]. NHEKs expressed a large amount of mRNAs for $P2Y_2$ receptors, but not for $P2Y_4$ or $P2Y_6$ receptors. All these pharmacological profiles showed that these responses should be mediated by $P2Y_2$ receptors (Figure 2). Very recently, Greig et al. [29] have reported that skin cells express P2X5, P2X7, $P2Y_1$ and $P2Y_2$ receptors, each of which is expressed in a spatially distinct zone of the epidermis and has distinct cellular functions. $P2Y_2$ receptors are expressed in the lower layer of the epidermis and are involved in proliferation, suggesting that the NHEKs used in the present study might mimic the basal cellular layer of skin cells *in vivo*.

The question remains as to whether endogenous ATP may produce propagating Ca^{2+} waves in NHEKs. Several reports have shown that mechanical stimulation produces a propagating Ca^{2+} wave in non-excitable cells such as astrocytes [15,30] and hepatocytes [12]. In astrocytes, extracellular molecules such as glutamate [11,31] and ATP [15,30], rather than gap junctions [32], are responsible for the propagation of Ca^{2+} waves. We sought to determine whether extracellular ATP produces intercellular Ca^{2+} waves in NHEKs. Mechanical stimulation of a single NHEK resulted in the induction of an intercellular Ca^{2+} wave, which was inhibited by the ATP-degrading enzyme, apyrase, and the P2 receptor antagonist, suramin (Figure 3). The gap junction inhibitor, 1-octanol, had little effect on the Ca^{2+} wave. Imaging of the ATP release by the modified luciferin–luciferase chemiluminescence clearly showed that the levels of extracellular ATP after mechanical stimulation were highest at the site of stimulation and decreased concentrically. These results strongly suggest that the mechanically evoked Ca^{2+} waves in NHEKs are mediated by extracellular ATP and by the activation of $P2Y_2$ receptors. As in astrocytes [15,30], extracellular ATP appears to play a pivotal role in creating the dynamic changes for long-range signalling in NHEKs.

The responses mediated by $P2Y_2$ receptors are probably layer-specific. The ATP-evoked hyperpolarization is very high in the basal layer but extremely low in the suprabasal layer in HaCaT keratinocytes [33]. The mRNA level of $P2Y_2$ receptors is down-regulated in differentiating HaCaT cells [34]. Thus the intercellular Ca^{2+} waves seen in the present study may be a response restricted to the basal layer of keratinocytes *in situ*. The finding that the barrier recovery rate of the mouse epidermis is regulated by functional P2 × 3 [35] suggests that the skin expresses multiple P2 receptors that are linked to distinct physiological functions.

There is an increasing body of evidence that ATP, the predominant extracellular signalling molecule of astrocytes [15,30], may also mediate signalling between neurons and glial cells [36–38]. With regard to the skin-to-sensory neuron system, a similar relationship may also be obtained. Especially, non-myelinated small-sized DRG neurons (nociceptors) terminate in the periphery as free nerve endings [39]. Thus nociceptors can directly contact skin-derived extracellular molecules when skin cells are injured, inflamed or otherwise stimulated. When cells are injured or destroyed, very high concentrations of intracellular ATP (> 5 mM) could leak and affect the surrounding NHEKs and DRG neurons. In the present study, however, we showed that the intercellular Ca^{2+} waves in NHEKs were reproducible when the same cell was stimulated repeatedly (Figure 6). Moreover, the increases in neuronal $[Ca^{2+}]_i$ in response to mechanical stimulation of NHEKs were also reproducible. Thus it appears that extracellular ATP-mediated NHEK-to-DRG neuron communication takes place even when cell damage is not involved. Somatic sensation requires the conversion of physical stimuli into depolarization of the distal nerve endings. It has been reported that activation of $P2Y_1$ receptors in sensory fibres increases the frequency of spikes evoked by a light touch of the skin [40]. Therefore the skin might sense and transmit non-harmful stimuli to sensory neurons via ATP.

DRG neurons express various types of P2 receptors. Ionotropic P2X receptors, especially P2X3 [41] and P2X2 [42] receptors in small- and middle-sized DRG neurons respectively, have been extensively studied in relation to pain. However, recent reports suggest that some P2Y receptors are present in small-sized DRG neurons and are involved in pain signalling. In small-sized neurons, activation of $P2Y_1$ or $P2Y_2$ receptors sensitizes TRPV1 receptors via protein kinase C-dependent mechanisms [43], stimulation of $P2Y_2$ receptors enhances the $[Ca^{2+}]$ increase, leading to the release of CGRP [44], and activation of $P2Y_2$

Figure 6 Dynamic communication between NHEKs and DRG neurons mediated by extracellular ATP

(**A**) Phase-contrast image (**a**) and pseudo colour $[Ca^{2+}]_i$ images (self-ratios of fluo-4 fluorescence; **b**–**f**) in co-cultured NHEKs and DRG neurons obtained by confocal laser microscopy. The white rectangle field in the middle of image **b** is shown enlarged in the bottom right of images **b**–**f**. The red arrowhead in image **b** depicts position 4 (DRG neuron 4). The white arrowhead in image **c** shows the initiation of Ca^{2+} wave in response to mechanical stimulation (cell 1). Scale bar, 50 μm. (**B**) The graph shows individual traces of the self-ratios of fluo-4 fluorescence in keratinocytes (K1–K3) and DRG neuron (N4) shown in image **Aa**. Keratinocyte 1 was mechanically stimulated twice (arrows S1 and S2) separated by 5 min. (**C**) Phase-contrast image (**a**) and pseudo colour $[Ca^{2+}]_i$ images (self-ratios of fluo-4 fluorescence; **b**–**f**) in co-cultured NHEKs and DRG neurons. The white rectangle field in the middle of image **b** is shown enlarged in the top right of images **b**–**f**. The red arrowhead in image **b** depicts position 4 (DRG neuron 4). The white arrowhead in image **c** shows the initiation of Ca^{2+} wave in response to mechanical stimulation (cell 1). Scale bar, 50 μm. (**D**) The graph shows individual traces of self-ratios of fluo-4 fluorescence in keratinocytes (K1–K3) and DRG neuron (N4) shown in image **a** in **C**. Keratinocyte 1 was mechanically stimulated twice (arrows S1 and S2) separated by 5 min. The first and second mechanical stimulations were performed in the absence and presence of 100 units/ml apyrase (grey horizontal bar).

receptors results in phosphorylation of CREB (cAMP-response-element-binding protein) [45]. We showed that approx. 70% of both small-sized DRG neurons and NHEKs possess functional $P2Y_2$ receptors in the co-culture (Figure 5). In the peripheral skin-to-sensory neuron system, $P2Y_2$ receptors might be the main sensor for both NHEKs and DRG neurons. However, we cannot exclude the possibility that Ca^{2+} entry via P2X receptors is also involved in Ca^{2+} signalling in DRG neurons. In fact, when skin cells are killed, a large amount of intracellular ATP in the skin leaks and excites nociceptors by activating P2X receptors [46]. In a skin–nerve preparation, carrageenan inflammation of skin resulted in an increase in the activities of c-fibres, which was mediated by P2X receptors [47]. There might be multiple mechanisms by which the skin communicates with sensory neurons through ATP.

Apart from those of cell injury, the mechanisms underlying ATP release from NHEKs remain unknown. In neuronal cells, depolarizing stimulation resulted in exocytotic release of ATP in hippocampal slices [48] and cultured hippocampal neurons [49]. However, in non-excitable cells including NHEKs, the mechanism of ATP release is still a matter of debate. In astrocytes, there have been several reports that ATP can be released via chloride channels [50], gap junction hemi-channels [51], ATP-binding cassette [52] and exocytosis [53,54]. NHEKs also express several types of chloride channels [34,55,56], connexins [57–59] and SNARE (soluble *N*-ethylmaleimide-sensitive fusion protein attachment protein receptor) proteins [60,61]. Although these similarities raise the possibility that NHEKs and astrocytes might share the same mechanism for the release of ATP, further investigation is needed.

In summary, we demonstrated that extracellular ATP derived from NHEKs functions in both an autocrine and paracrine manner in the peripheral skin-to-sensory neurons system. Metabotropic $P2Y_2$ receptors may be important sensors for extracellular ATP in both NHEKs and small-sized DRG neurons.

We thank T. Obama (Division of Biosignaling, National Institute of Health Sciences) for helping in the culturing of cells and Y. Ohno (Division of Pharmacology, National Institute of Health Sciences) for continuous encouragement. This work was partially supported by the Organization for Pharmaceutical Safety and Research (Medical Frontier Project; MF-16), the Health Science Foundation (Japan) and Shiseido Research Center (Yokohama, Japan).

REFERENCES

1 Denda, M., Fuziwara, S., Inoue, K., Denda, S., Akamatsu, H., Tomitaka, A. and Matsunaga, K. (2001) Immunoreactivity of VR1 on epidermal keratinocyte of human skin. Biochem. Biophys. Res. Commun. **285**, 1250–1252

2 Inoue, K., Koizumi, S., Fuziwara, S., Denda, S. and Denda, M. (2002) Functional vanilloid receptors in cultured normal human epidermal keratinocytes. Biochem. Biophys. Res. Commun. **291**, 124–129

3 Grando, S. A. (1997) Biological functions of keratinocyte cholinergic receptors. J. Investig. Dermatol. Symp. Proc. **2**, 41–48

4 Arredondo, J., Nguyen, V. T., Chernyavsky, A. I., Bercovich, D., Orr-Urtreger, A., Kummer, W., Lips, K., Vetter, D. E. and Grando, S. A. (2002) Central role of α7 nicotinic receptor in differentiation of the stratified squamous epithelium. J. Cell Biol. **159**, 325–336

5 Genever, P. G., Maxfield, S. J., Kennovin, G. D., Maltman, J., Bowgen, C. J., Raxworthy, M. J. and Skerry, T. M. (1999) Evidence for a novel glutamate-mediated signaling pathway in keratinocytes. J. Invest. Dermatol. **112**, 337–342

6 Dixon, C. J., Bowler, W. B., Littlewood-Evans, A., Dillon, J. P., Bilbe, G., Sharpe, G. R. and Gallagher, J. A. (1999) Regulation of epidermal homeostasis through P2Y2 receptors. Br. J. Pharmacol. **127**, 1680–1686

7 Stoebner, P. E., Carayon, P., Penarier, G., Frechin, N., Barneon, G., Casellas, P., Cano, J. P., Meynadier, J. and Meunier, L. (1999) The expression of peripheral benzodiazepine receptors in human skin: the relationship with epidermal cell differentiation. Br. J. Dermatol. **140**, 1010–1016

8 Zia, S., Ndoye, A., Lee, T. X., Webber, R. J. and Grando, S. A. (2000) Receptor-mediated inhibition of keratinocyte migration by nicotine involves modulations of calcium influx and intracellular concentration. J. Pharmacol. Exp. Ther. **293**, 973–981

9 Watt, F. M., Hudson, D. L., Lamb, A. G., Bolsover, S. R., Silver, R. A., Aitchison, M. J. and Whitaker, M. (1991) Mitogens induce calcium transients in both dividing and terminally differentiating keratinocytes. J. Cell Sci. **99**, 397–405

10 Cornell-Bell, A. H., Finkbeiner, S. M., Cooper, M. S. and Smith, S. J. (1990) Glutamate induces calcium waves in cultured astrocytes: long-range glial signaling. Science **247**, 470–473

11 Charles, A. C., Merrill, J. E., Dirksen, E. R. and Sanderson, M. J. (1991) Intercellular signaling in glial cells: calcium waves and oscillations in response to mechanical stimulation and glutamate. Neuron **6**, 983–992

12 Thomas, A. P., Renard, D. C. and Rooney, T. A. (1991) Spatial and temporal organization of calcium signalling in hepatocytes. Cell Calcium **12**, 111–126

13 Hansen, M., Boitano, S., Dirksen, E. R. and Sanderson, M. J. (1993) Intercellular calcium signaling induced by extracellular adenosine 5′-triphosphate and mechanical stimulation in airway epithelial cells. J. Cell Sci. **106**, 995–1004

14 Demer, L. L., Wortham, C. M., Dirksen, E. R. and Sanderson, M. J. (1993) Mechanical stimulation induces intercellular calcium signaling in bovine aortic endothelial cells. Am. J. Physiol. **264**, H2094–H2102

15 Guthrie, P. B., Knappenberger, J., Segal, M., Bennett, M. V., Charles, A. C. and Kater, S. B. (1999) ATP released from astrocytes mediates glial calcium waves. J. Neurosci. **19**, 520–528

16 Scemes, E., Dermietzel, R. and Spray, D. C. (1998) Calcium waves between astrocytes from Cx43 knockout mice. Glia **24**, 65–73

17 Cauna, N. (1973) The free penicillate nerve endings of the human hairy skin. J. Anat. **115**, 277–288

18 Hilliges, M., Wang, L. and Johansson, O. (1995) Ultrastructural evidence for nerve fibers within all vital layers of the human epidermis. J. Invest. Dermatol. **104**, 134–137

19 Peier, A. M., Reeve, A. J., Andersson, D. A., Moqrich, A., Earley, T. J., Hergarden, A. C., Story, G. M., Colley, S., Hogenesch, J. B., McIntyre, P. et al. (2002) A heat-sensitive TRP channel expressed in keratinocytes. Science **296**, 2046–2049

20 Hensel, H. and Iggo, A. (1971) Analysis of cutaneous warm and cold fibres in primates. Pflugers Arch. **329**, 1–8

21 Hensel, H. and Kenshalo, D. R. (1969) Warm receptors in the nasal region of cats. J. Physiol. (Cambridge, U.K.) **204**, 99–112

22 Grynkiewicz, G., Poenie, M. and Tsien, R. Y. (1985) A new generation of Ca^{2+} indicators with greatly improved fluorescence properties. J. Biol. Chem. **260**, 3440–3450

23 Koizumi, S., Rosa, P., Willars, G. B., Challiss, R. A., Taverna, E., Francolini, M., Bootman, M. D., Lipp, P., Inoue, K., Roder, J. et al. (2002) Mechanisms underlying the neuronal calcium sensor-1-evoked enhancement of exocytosis in PC12 cells. J. Biol. Chem. **277**, 30315–30324

24 Koizumi, S., Bootman, M. D., Bobanovic, L. K., Schell, M. J., Berridge, M. J. and Lipp, P. (1999) Characterization of elementary Ca^{2+} release signals in NGF-differentiated PC12 cells and hippocampal neurons. Neuron **22**, 125–137

25 Communi, D., Pirotton, S., Parmentier, M. and Boeynaems, J. M. (1995) Cloning and functional expression of a human uridine nucleotide receptor. J. Biol. Chem. **270**, 30849–30852

26 Chang, K., Hanaoka, K., Kumada, M. and Takuwa, Y. (1995) Molecular cloning and functional analysis of a novel P2 nucleotide receptor. J. Biol. Chem. **270**, 26152–26158

27 Communi, D., Parmentier, M. and Boeynaems, J. M. (1996) Cloning, functional expression and tissue distribution of the human P2Y6 receptor. Biochem. Biophys. Res. Commun. **222**, 303–308

28 Communi, D., Motte, S., Boeynaems, J. M. and Pirotton, S. (1996) Pharmacological characterization of the human P2Y4 receptor. Eur. J. Pharmacol. **317**, 383–389

29 Greig, A. V., Linge, C., Terenghi, G., McGrouther, D. A. and Burnstock, G. (2003) Purinergic receptors are part of functional signaling system for proliferation and differentiation of human epidermis keratinocytes. J. Invest. Dermatol. **120**, 1007–1015

30 Fam, S. R., Gallagher, C. J. and Salter, M. W. (2000) P2Y1 purinoceptor-mediated Ca^{2+} signaling and Ca^{2+} wave propagation in dorsal spinal cord astrocytes. J. Neurosci. **20**, 2800–2808

31 Newman, E. A. and Zahs, K. R. (1998) Modulation of neuronal activity by glial cells in the retina. J. Neurosci. **18**, 4022–4028

32 Finkbeiner, S. (1992) Calcium waves in astrocytes – filling in the gaps. Neuron **8**, 1101–1108

33 Burgstahler, R., Koegel, H., Rucker, F., Tracey, D., Grafe, P. and Alzheimer, C. (2003) Confocal ratiometric voltage imaging of cultured human keratinocytes reveals layer-specific responses to ATP. Am. J. Physiol. **284**, C944–C952

34 Koegel, H. and Alzheimer, C. (2001) Expression and biological significance of Ca^{2+}-activated ion channels in human keratinocytes. FASEB J. **15**, 145–154

35 Denda, M., Inoue, K., Fuziwara, S. and Denda, S. (2002) P2X purinergic receptor antagonist accelerates skin barrier repair and prevents epidermal hyperplasia induced by skin barrier disruption. J. Invest. Dermatol. **119**, 1034–1040
36 Koizumi, S., Fujishita, K., Tsuda, M., Shigemoto-Mogami, Y. and Inoue, K. (2003) Dynamic inhibition of excitatory synaptic transmission by astrocyte-derived ATP in hippocampal cultures. Proc. Natl. Acad. Sci. U.S.A. **100**, 11023–11028
37 Newman, E. A. (2003) Glial cell inhibition of neurons by release of ATP. J. Neurosci. **23**, 1659–1666
38 Tsuda, M., Shigemoto-Mogami, Y., Koizumi, S., Mizokoshi, A., Kohsaka, S., Salter, M. W. and Inoue, K. (2003) P2X4 receptors induced in spinal microglia gate tactile allodynia after nerve injury. Nature (London) **424**, 778–783
39 Cervero, F. (1994) Sensory innervation of the viscera: peripheral basis of visceral pain. Physiol. Rev. **74**, 95–138
40 Nakamura, F. and Strittmatter, S. M. (1996) P2Y1 purinergic receptors in sensory neurons: contribution to touch-induced impulse generation. Proc. Natl. Acad. Sci. U.S.A. **93**, 10465–10470
41 Burnstock, G. (2000) P2X receptors in sensory neurones. Br. J. Anaesth. **84**, 476–488
42 Tsuda, M., Koizumi, S., Kita, A., Shigemoto, Y., Ueno, S. and Inoue, K. (2000) Mechanical allodynia caused by intraplantar injection of P2X receptor agonist in rats: involvement of heteromeric P2X2/3 receptor signaling in capsaicin-insensitive primary afferent neurons. J. Neurosci. **20**, RC90
43 Tominaga, M., Wada, M. and Masu, M. (2001) Potentiation of capsaicin receptor activity by metabotropic ATP receptors as a possible mechanism for ATP-evoked pain and hyperalgesia. Proc. Natl. Acad. Sci. U.S.A. **98**, 6951–6956
44 Sanada, M., Yasuda, H., Omatsu-Kanbe, M., Sango, K., Isono, T., Matsuura, H. and Kikkawa, R. (2002) Increase in intracellular Ca^{2+} and calcitonin gene-related peptide release through metabotropic P2Y receptors in rat dorsal root ganglion neurons. Neuroscience **111**, 413–422
45 Molliver, D. C., Cook, S. P., Carlsten, J. A., Wright, D. E. and McCleskey, E. W. (2002) ATP and UTP excite sensory neurons and induce CREB phosphorylation through the metabotropic receptor, P2Y2. Eur. J. Neurosci. **16**, 1850–1860
46 Cook, S. P. and McCleskey, E. W. (2002) Cell damage excites nociceptors through release of cytosolic ATP. Pain **95**, 41–47
47 Hamilton, S. G., McMahon, S. B. and Lewin, G. R. (2001) Selective activation of nociceptors by P2X receptor agonists in normal and inflamed rat skin. J. Physiol. (Cambridge, U.K.) **534**, 437–445

Received 21 July 2003/23 December 2003; accepted 16 February 2004
Published as BJ Immediate Publication 16 February 2004, DOI 10.1042/BJ20031089

48 Wieraszko, A., Goldsmith, G. and Seyfried, T. N. (1989) Stimulation-dependent release of adenosine triphosphate from hippocampal slices. Brain Res. **485**, 244–250
49 Koizumi, S., Fujishita, K., Tsuda, M. and Inoue, K. (2003) Neuron-to-astrocyte communication by endogenous ATP in mixed culture of rat hippocampal neurons and astrocyte. Drug Dev. Res. **59**, 88–94
50 Darby, M., Kuzmiski, J. B., Panenka, W., Feighan, D. and MacVicar, B. A. (2003) ATP released from astrocytes during swelling activates chloride channels. J. Neurophysiol. **89**, 1870–1877
51 Stout, C. E., Costantin, J. L., Naus, C. C. and Charles, A. C. (2002) Intercellular calcium signaling in astrocytes via ATP release through connexin hemichannels. J. Biol. Chem. **277**, 10482–10488
52 Ballerini, P., Di Iorio, P., Ciccarelli, R., Nargi, E., D'Alimonte, I., Traversa, U., Rathbone, M. P. and Caciagli, F. (2002) Glial cells express multiple ATP binding cassette proteins which are involved in ATP release. Neuroreport **13**, 1789–1792
53 Maienschein, V., Marxen, M., Volknandt, W. and Zimmermann, H. (1999) A plethora of presynaptic proteins associated with ATP-storing organelles in cultured astrocytes. Glia **26**, 233–244
54 Coco, S., Calegari, F., Pravettoni, E., Pozzi, D., Taverna, E., Rosa, P., Matteoli, M. and Verderio, C. (2003) Storage and release of ATP from astrocytes in culture. J. Biol. Chem. **278**, 1354–1362
55 Galietta, L. J., Barone, V., de Luca, M. and Romeo, G. (1991) Characterization of chloride and cation channels in cultured human keratinocytes. Pflugers Arch. **418**, 18–25
56 Mastrocola, T., de Luca, M. and Rugolo, M. (1991) Characterization of chloride transport pathways in cultured human keratinocytes. Biochim. Biophys. Acta **1097**, 275–282
57 Risek, B. and Gilula, N. B. (1991) Spatiotemporal expression of three gap junction gene products involved in fetomaternal communication during rat pregnancy. Development **113**, 165–181
58 Di, W. L., Rugg, E. L., Leigh, I. M. and Kelsell, D. P. (2001) Multiple epidermal connexins are expressed in different keratinocyte subpopulations including connexin 31. J. Invest. Dermatol. **117**, 958–964
59 Plum, A., Hallas, G. and Willecke, K. (2002) Expression of the mouse gap junction gene Gjb3 is regulated by distinct mechanisms in embryonic stem cells and keratinocytes. Genomics **79**, 24–30
60 Scott, G. and Zhao, Q. (2001) Rab3a and SNARE proteins: potential regulators of melanosome movement. J. Invest. Dermatol. **116**, 296–304
61 Scott, G., Leopardi, S., Printup, S. and Madden, B. C. (2002) Filopodia are conduits for melanosome transfer to keratinocytes. J. Cell Sci. **115**, 1441–1451